Optimization and Sensitivity Analysis of Numerical Simulation of Tubular Hydroforming

Honggang An and Daniel E. Green
Dept. of Mechanical, Automotive and Materials Engineering,
University of Windsor, 401 Sunset Avenue, Windsor, N9B 3P4, Ontario, Canada

Abstract

Optimization and sensitivity analysis is important although difficult to obtain for tubular hydroforming, because of the implicit relationship between the load path variables (internal pressure and tube end displacement) and the dependent variables (such as stress, strain and final tube thickness). In this paper, the Taguchi method was used in conjunction with virtual hydroforming experiments using LS-DYNA® to carry out the sensitivity analysis and optimization of straight-tube hydroforming. This method employs an orthogonal array to study a large parameter space using only a small number of numerical simulations. Since the tube wall undergoes bending as it fills the corner of the die during the final stage of hydroforming, the strain path becomes non-linear. In this situation, the traditional strain forming limit diagram (FLD) is not a reliable criterion for necking/fracture. In contrast, the forming limit stress diagram (FLSD) is practically strain path-independent. Therefore, the FLSD was adopted for the necking/fracture criterion of the process. Multi-objective functions that consider necking/fracture, wrinkling and severe thinning were taken to evaluate the performance of each simulation. The Pareto optimum was obtained with a minimum failure value using the minimum distance method. Furthermore, the analysis of variance (ANOVA) statistical method was used to determine the effects of the forming parameters on the quality of the final hydroformed part. The factor response was completed using the Signal-to-Noise (S/N) ratio and ANOVA results. The ANOVA indicates the degree of sensitivity for the hydroforming parameters, and expansion pressure, calibration pressure, and tube end displacement were shown to be the three most important factors. This combination of numerical analyses and an optimization technique has helped to define a load path that leads to a robust manufacturing process and good part quality.
***Keywords**: Tube hydroforming, FLSD, Taguchi method, Sensitivity analysis, Pareto optimization*

Introduction

To fully understand and correctly carry out tube hydroforming, it is advantageous to investigate the sensitivity of the tube response to variations in geometrical dimensions, material properties and load path. Since there is no explicit relationship between forming severity and load path, it is very difficult to perform a sensitivity analysis by analytical methods. Physical experimental methods would be very expensive and sometimes impossible. Numerical simulation can be an effective and less expensive way to carry out the sensitivity analysis.

The Taguchi method has been proved to be effective in experimental design in a variety of industrial applications. It employs an orthogonal array to study a large parameter space using only a small number of experiments [1-2]. Another benefit of the Taguchi approach is that it determines the relative contribution of each factor to process reliability by the analysis of variance (ANOVA) statistical method. This allows design efforts to be concentrated on the most sensitive factors.

Manabe et al. [3] carried out experiments using a computer-controlled testing apparatus to examine the influence of linear and non-linear loading paths on the behavior of thin-walled

aluminum tubes during hydroforming. Manabe [4] also confirmed the factors that affect wall thickness distribution of the hydroformed part by finite element (FE) simulation and experimental work. MacDonald [5] performed a finite element simulation of the hydroforming of cross-joints from straight tubes, to investigate the effects of various process parameters using the bulge forming method. Ray et al. [6] determined the optimal load paths using FE simulations and a load control algorithm for X- and T-branch tube hydroforming processes by maximizing the part expansion and simultaneously maintaining wall thickness, forming stresses and plastic strains within the allowable limits. Li et al. [7, 8] developed a method to analyze the effects of the forming parameters on the uniformity of tube wall thickness by using the Taguchi method and finite element analysis (FEA) and determined the optimal combination of the forming parameters for the process. However, the influence of load path was not investigated since this study did not include end feeding.

This work consisted of investigating the formability characteristics of straight, hydroformed tubes using the explicit FEA code LS-DYNA® [9]. In addition, the Taguchi method was combined with FE simulations to optimize the load path through Pareto multi-objective optimization. The sensitive factors of load path were identified with the ANOVA method. Meanwhile, FLSD and FLD were both used to evaluate the risk of necking or fracture, of wrinkling and severe thinning, separately.

Virtual Experiments and FEA Simulation

Finite Element Model with LS-DYNA

In this study, straight tube hydroforming was simulated under different load paths. Fig.1 shows the FE model set up with LS-DYNA.

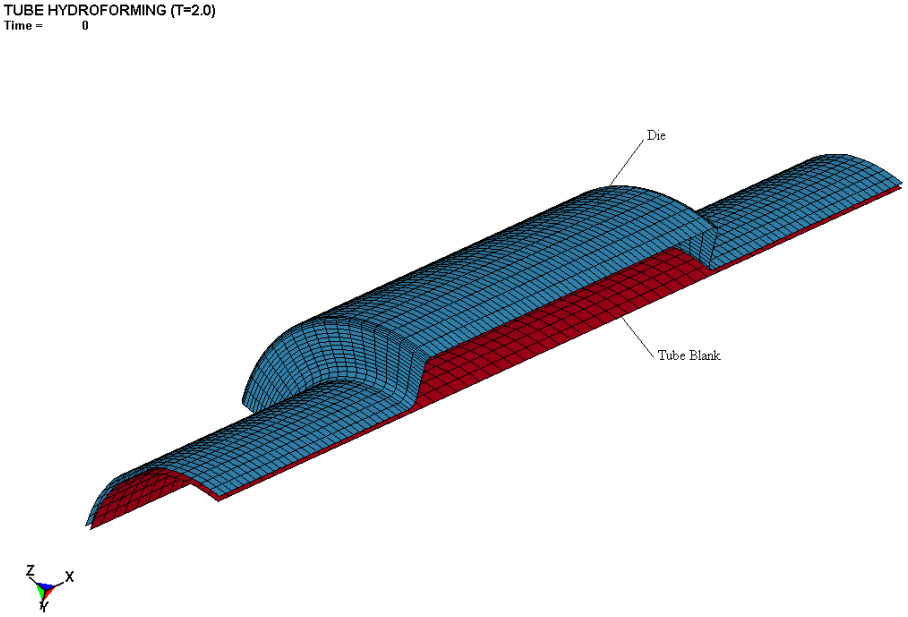

Fig.1 One quarter of the FE model of straight tube hydroforming (LS-DYNA)

The die surface was considered to be rigid. The as-received tube was made of mild steel and was modeled using Belytschko-Tsay shell elements, with 7 integration points through the thickness.

The tube was assigned a material model of "*MAT_ PIECEWISE_ LINEAR_PLASTICITY". Due to the symmetry, only 1/4 of the die and tube were modeled and symmetric boundary conditions were applied along the boundary planes. There were 4185 nodes and 3600 shell elements, i.e. 900 elements for the tube and 2700 elements for the die. An internal pressure was applied to the tube according to the load curve shown in Fig. 2. The end feed was applied to the both ends of the tube node sets. Finally, the coefficient of friction for contact interface between the tube and the die was set to $\mu = 0.1$.

Virtual Experiment Design of Load Path

Imaninejad et al. [10] and Al-Qureshi & Moriera Filho. [11] have concluded that increasing the number of load path segments approximating the optimum load curve not only increases the computational efficiency but also produces final components with a more uniform thickness distribution and/or larger bulge heights. Therefore, the load path for straight-tube hydroforming was constructed with four parameters: P1, P2, and P3 which are three levels of internal pressure (and correspond with the pre-expansion, expansion and calibration stages) and D, the displacement applied at the tube ends. Accordingly, a five-stage path was chosen for the internal pressure in the current study (Fig. 2). The total simulation time was 0.005s.

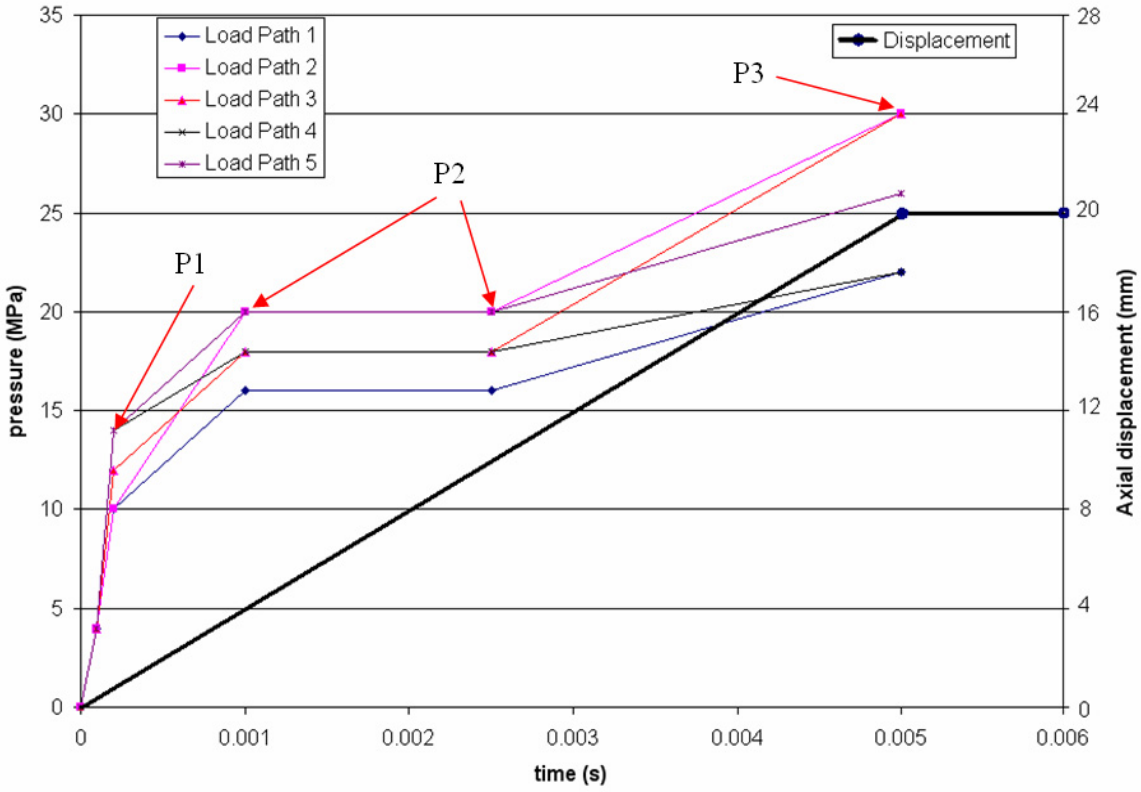

Fig. 2 Piecewise linear load curve

An orthogonal array ($L_9(3^4)$) was chosen for the virtual experiments (Table 1).

A batch mode method was used to output the strains and stresses in LS-PREPOST (Fig.3). All the output commands were included in the command file which made output operations very simple. This was very useful especially when the analysis required a large number of output

tasks: for example, to output and track the strain path of the critical element from stage 0 to stage 27 in the current study.

Table 1 $L_9(3^4)$ Orthogonal array

Run No.	P1(MPa)	P2(MPa)	P3(MPa)	end feed D (mm)
1	10	16	22	12
2	10	18	26	16
3	10	20	30	20
4	12	16	26	20
5	12	18	30	12
6	12	20	22	16
7	14	16	30	16
8	14	18	22	20
9	14	20	26	10

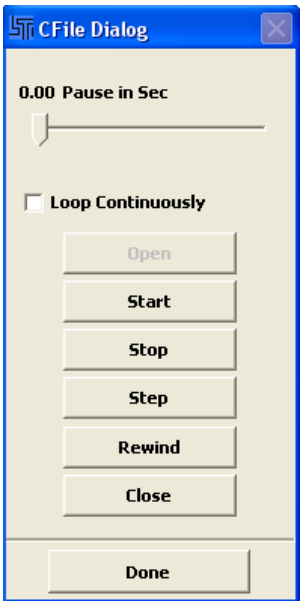

Fig. 3 LS-PREPOST command file module

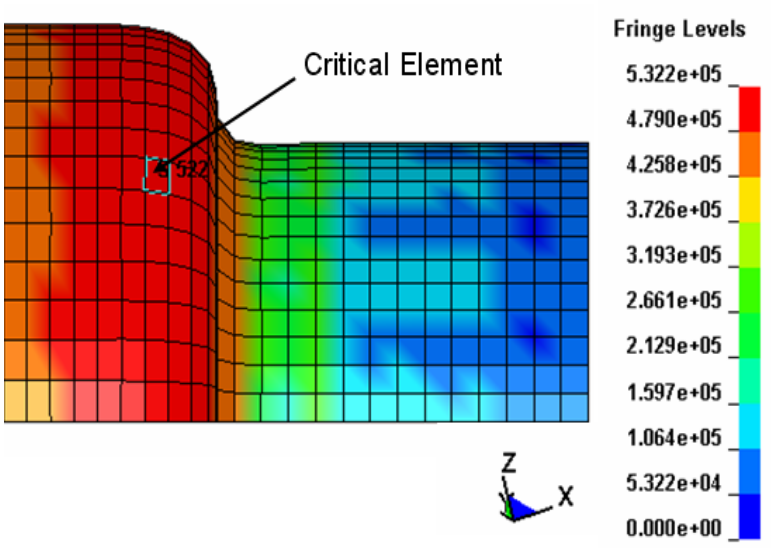

Fig.4 Critical Element with maximum stress

Forming limit stress diagram

The hydroforming simulations showed (Fig. 4 & 5) that the strain path in the critical element (i.e. the element with the maximum stress at the mid-plane of the tube wall) was non-linear regardless of the loading conditions. The tube wall actually undergoes bending as it fills the corner of the die during the final stage of hydroforming, thus causing the strain path to become non-linear. In this situation, the traditional strain forming limit diagram (FLD) is not a reliable failure criterion. Stoughton [12] proposed to evaluate the forming severity of components formed with non-linear strain paths using a stress-based failure criterion. Yoshida et al. [13] have shown that the forming limit stress diagram (FLSD) is indeed practically strain-path independent. Therefore, the FLSD failure criterion was adopted for the process optimization.

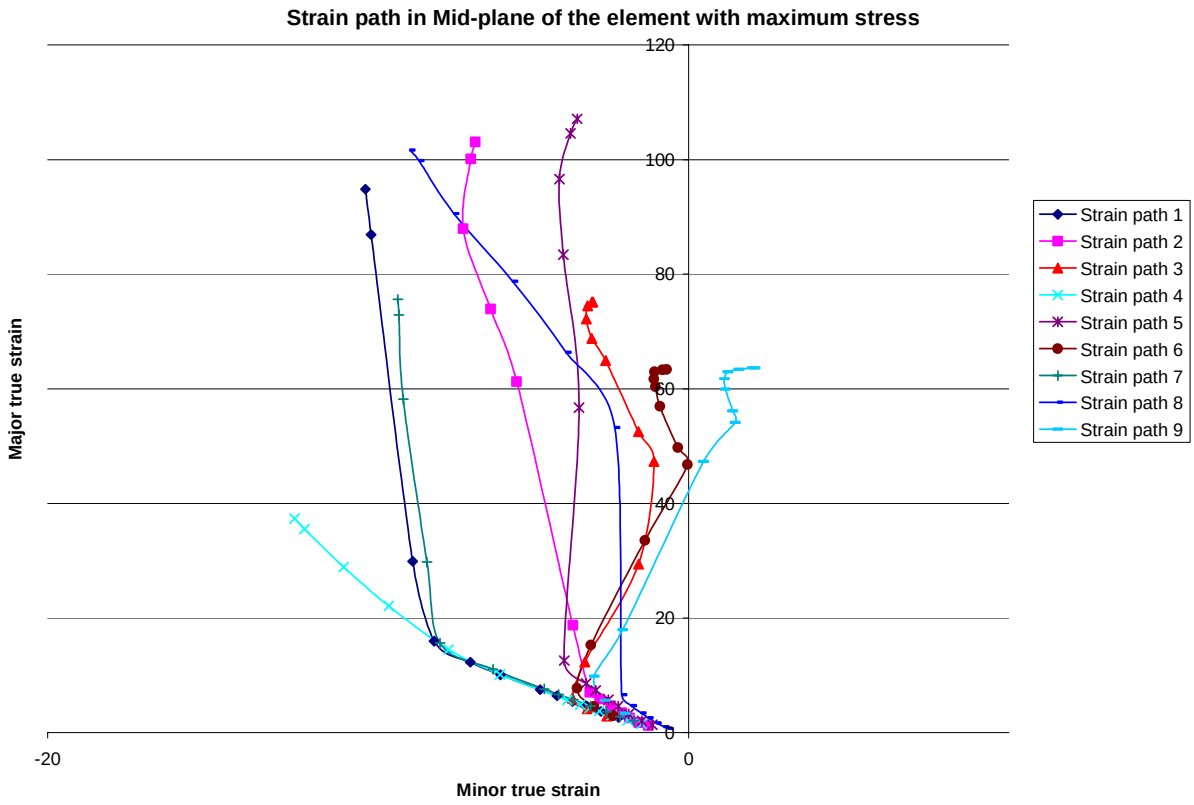

Fig.5 Predicted strain paths in the most critical element (maximum stress) for each loading condition

Failure criterion considering necking/fracture, wrinkling and severe thinning

FLSD has been shown to be a more appropriate failure criterion for metal forming processes which lead to non-linear strain paths [12, 14, 15, 16]. Furthermore, Stoughton & Yoon [17] pointed out that the most critical stress states attained during the forming simulation ought to be evaluated against the FLSD, and not merely the stress states recorded for post-processing purposes. Therefore, in order to take account for the widest range of possible failures, a multi-objective failure criterion was adopted to evaluate the effects of load path. The types of failures considered were, necking or splitting in the tube wall, wrinkling and severe thinning.

The objective functions were taken to be the difference (i.e. d_f) between the maximum stress and the corresponding FLSD, as well as the sum of the square of the difference (i.e. d_w and d_{th}) between the major strain and the wrinkling and severe thinning curve in FLD as following equations (1-6), where the notation i (i=1, 2, ...n) is the element number, and n is the total number of elements in the tube.

Objective function for necking or fracture:

$$Obj\_f = d_f = Max\left|\sigma_1^i - \sigma_f^i\right| \qquad (1)$$

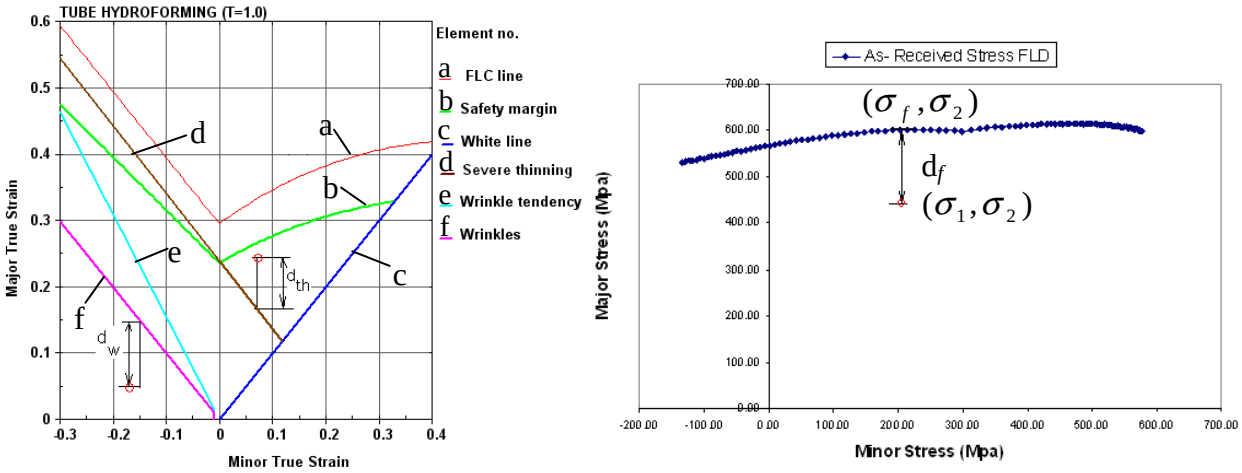

a. Strain FLD b. As-received FLSD

Fig. 6 Definition of the objective functions

Where σ_1 is the numerically calculated principal stress in element *i* and σ_f is the corresponding forming stress limit. The optimization will seek to maximize this objective function because a larger distance signifies a lesser tendency for fracture. However, for the sake of convenience, Eq. (1) can be rewritten as Eq. (2) and will be minimized.

$$Obj\_f = \frac{1}{d_f} = \frac{1}{Max\left|\sigma_1^i - \sigma_f^i\right|} \tag{2}$$

Objective function for wrinkling:

$$\begin{cases} Obj\_w = \sum_{i=1}^{n} (d_w^i)^2 = \sum_{i=1}^{n} \left(\varepsilon_1^i - \varepsilon_w^i\right)^2 & \varepsilon_1^i < \varphi(\varepsilon_2^i) \\ Obj\_w = 0 & \varepsilon_1^i \geq \varphi(\varepsilon_2^i) \end{cases} \tag{3}$$

$$\varepsilon_w = \varphi(\varepsilon_2) \tag{4}$$

Where ε_1 is the major strain in element *i*, and ε_w is the wrinkling limit value determined from the FLD curve f (Fig. 6a), which is defined by Eq. (4).

Objective function for severe thinning:

$$\begin{cases} Obj\_th = \sum_{i=1}^{n} (d_{th}^i)^2 = \sum_{i=1}^{n} \left(\varepsilon_1^i - \phi(\varepsilon_2^i)\right)^2 & \varepsilon_1^i > \phi(\varepsilon_2^i) \\ Obj\_th = 0 & \varepsilon_1^i \leq \phi(\varepsilon_2^i) \end{cases} \tag{5}$$

$$\varepsilon_{th} = \phi(\varepsilon_2) \tag{6}$$

Where ε_1 is the major strain in element *i*, and ε_{th} is the thinning limit determined from the FLD curve d (Fig. 6a), which is defined by Eq. (6). The above optimization endeavors to determine the minimum value of each of these objective functions.

Results and Analysis

For multi-objective problems, different objectives have different magnitudes and units, and it is not possible to evaluate the quality of the simulated tubes directly from the objective function values. Therefore, after obtaining the results for each virtual experiment, the objective values were normalized to a dimensionless value between 0 and 1 (Table 2).

The normalization method can be described as follows: each objective value was scaled with the average value and suitable lower and upper bounds were selected to normalize the value within the range [0,1]. The following formulae were used for this normalization procedure:

$$N_f = \left(\frac{Obj\_f}{Obj\_f_{avg}} - l_f\right)\left(\frac{1}{u_f - l_f}\right)$$
$$N_w = \left(\frac{Obj\_w}{Obj\_w_{avg}} - l_w\right)\left(\frac{1}{u_w - l_w}\right) \quad (7)$$
$$N_{th} = \left(\frac{Obj\_th}{Obj\_th_{avg}} - l_{th}\right)\left(\frac{1}{u_{th} - l_{th}}\right)$$

where N_f ,N_w and N_{th} are the normalized values of objective of necking/fracture, wrinkling and severe thinning, respectively. Obj_f_{avg}, Obj_w_{avg} and Obj_th_{avg} are the average values of the three objective functions. l_f, l_w, l_{th}, u_f, u_w and u_{th} are the lower and upper bounds selected above. Although there are various ways to normalize these objective functions, the normalization method does not actually affect the Pareto ranking.

After the objective functions were determined, the Signal-to-Noise ratio was also calculated for each run, as follows:

$$S/N = -10\log\left(\frac{y_i^{\,2}}{n}\right) \quad (8)$$

Where y_i are the normalized values of the three objectives (Table 2), and n is the number of repeat tests (n = 1 in this study). Regardless of the definition of the S/N, a greater S/N ratio always corresponds to better quality characteristic.

Table 2 Factor responses and S/N ratio for each objective

Run No.	*Obj_f* (fracture) (10^{-5})	*Obj_w* (wrinkling) (10^{-5})	*Obj_th* (severe thinning)	Normalization			S/N ratio		
				Fracture	Wrinkling	Severe thinning	Fracture	Wrinkling	thinning
1	2.6870	0	421.22	0.7036	0.0000	0.2667	3.05	N/A	11.48
2	2.1379	50.606	758.70	0.4917	0.0739	0.4804	6.17	22.62	6.37
3	1.3617	551.57	415.29	0.1922	0.8057	0.2630	14.33	1.88	11.60
4	1.2027	280.48	86.13	0.1308	0.4097	0.0545	17.67	7.75	25.27
5	2.4980	0	1189.18	0.6307	0.0000	0.7530	4.00	N/A	2.46
6	1.5476	527.26	312.79	0.2639	0.7702	0.1981	11.57	2.27	14.06
7	1.9502	181.82	339.03	0.4193	0.2656	0.2147	7.55	11.52	13.36
8	1.5974	457.59	872.23	0.2831	0.6684	0.5523	10.96	3.50	5.16
9	1.6158	4.4637	342.92	0.2902	0.0065	0.2172	10.75	43.71	13.26

Pareto set 1 includes Runs No. 2, 4, 7 and 9, Pareto set 2 includes Runs No. 3, 4, 6 and 9 and Pareto set 3 includes Runs No. 1, 2, 4, 7 and 9 (see Fig.7-9). From the three Pareto sets, there are 2 load paths (Run No. 4 and 9) that appear to be optimum. However, considering that the load path for run No.9 may result in necking/fracture and severe thinning, the overall optimal result is considered to be Run No. 4. The load path for this simulation is determined by P1=12 MPa, P2=16 MPa, P3=26 MPa and end feed D=20mm.

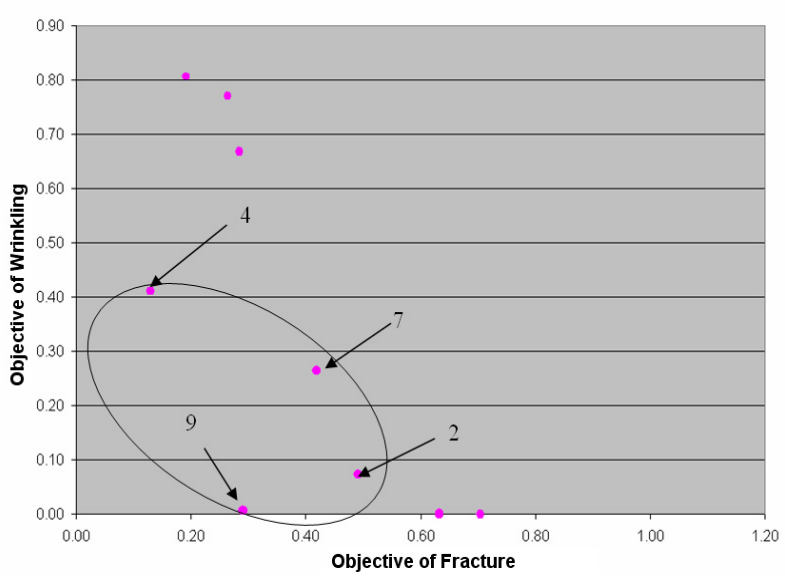

Fig. 7 Pareto set 1 (Fracture and wrinkling)

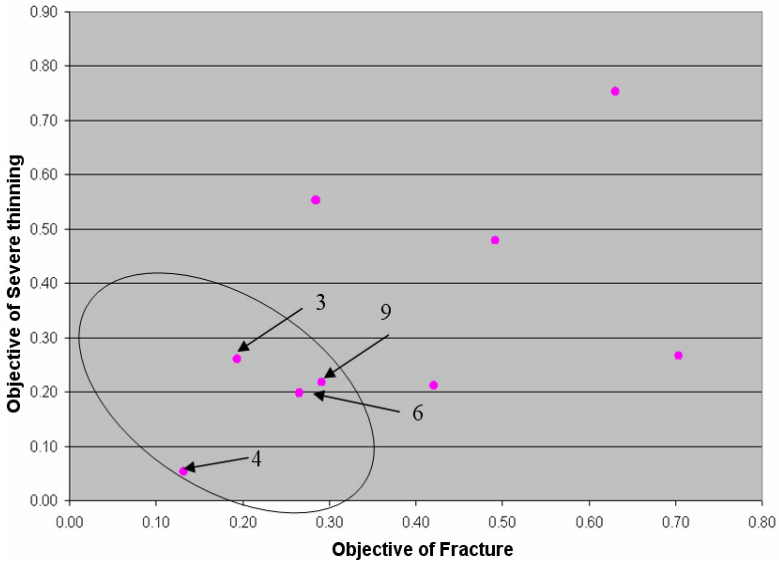

Fig. 8 Pareto set 2 (Fracture and severe thinning)

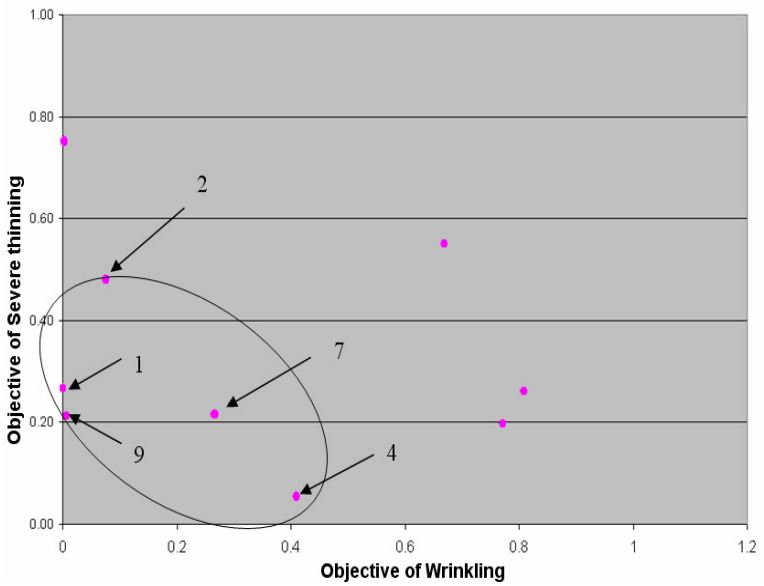

Fig.9 Pareto set 3 (wrinkling and severe thinning)

By an analysis of variance (ANOVA), it can be seen (from the sum of squares or F-ratio) in Tables 3 and 4 that D, P2 and P3 are the three most critical factors for necking/fracture, while P2, P3 and D are the three most significant variables for severe thinning.

Table 3 Analysis of variance for fracture

	Level 1	Level 2	Level 3	Degree of freedom	Sum of squares	Mean sq	F ratio
P1	7.848	**11.080**	9.752	2.000	15.83	7.917	0.565
P2	9.423	7.043	**12.214**	2.000	40.19	20.093	1.435
P3	8.528	**11.526**	8.627	2.000	17.40	8.702	0.621
end feed D	5.934	8.429	**14.318**	2.000	111.19	55.595	3.970
Error	Pool P1-P2						
Total				8.000	184.613		
Pooled error				4.000	56.019	14.005	

Table 4 Analysis of variance for severe thinning

	Level 1	Level 2	Level 3	Degree of freedom	Sum of squares	Mean sq	F ratio
P1	9.816	**13.931**	10.595	2.000	28.67	14.334	0.223
P2	**16.702**	4.662	12.977	2.000	227.98	113.989	1.777
P3	10.233	**14.966**	9.143	2.000	57.49	28.746	0.448
end feed D	9.069	11.265	**14.007**	2.000	36.73	18.367	0.286
Error	Pool P1-P2						
Total				8.000	350.874		
Pooled error				4.000	256.647	64.162	

For the three objectives combined (necking/fracture, wrinkling and severe thinning), P2 was the most significant factor, and D and P3 were shown to be the next most sensitive factors for THF simulation.

When considering only the risk of fracture, the ANOVA showed that the optimal combination of P1 (level 2), P2 (level 3), P3 (level 2) and end feed D (level 3) was layout 2323 (values highlighted in bold in Table 3). However for severe thinning, it was shown that 2123 is the optimal layout. Consequently, layout 2123 was the optimum layout for the load path, both in terms of the analysis of Pareto optimum and the analysis of variance. Finally, since the optimal load path parameters obtained above coincided with Run No. 4, no further experimental confirmation was needed.

It can also be observed in Figure 5, that the strain path in the critical element for the simulation with this optimal load path (strain path No.4) is significantly improved compared to the strain paths obtained with other load paths.

It may be pointed out that the influence of interactions between the factors in orthogonal array (L_9) was not considered in this study. If more computational resources (CPU time and memory) are required, an L_{18} orthogonal array may be a better option to minimize the interactions.

Conclusions

LS-DYNA is a powerful numerical tool that was combined with the Taguchi method and Pareto optimization in order to optimize the load path for tube hydroforming applications. In addition, an analysis of variance was used to determine the sensitivity of the hydroforming process to the various parameters that define the load path. The case study of straight tube has shown the following:

(1) The multi-objective optimization in conjunction with Taguchi method and analysis of variance can not only provide a way to obtain the optimum load path for virtual experiments, but also carry out the sensitivity analysis with statistical ANOVA method. It was shown that the expansion pressure (P2), the calibration pressure (P3) and the tube end displacement (D) are the most significant factors in tube hydroforming. Furthermore, the expansion pressure (P2) was shown to have a stronger effect on the forming severity of tubular parts than the other two factors.

(2) The FLD and the FLSD were found to be very useful in evaluating the effect of load path on the forming severity of hydroformed parts. However, it was also pointed out that they need to be used by taking the advantage of each other.

(3) The optimal load path (Run No. 4) was shown to have generated a significantly improved strain path for the critical element compared to the other strain paths.

It is also worth pointing out that, while this optimization procedure was applied to a very simple case study (i.e. expansion of a straight tube), it is also applicable to more complex, industrial hydroforming applications.

References

[1] Taguchi, G., System of Experimental Design, UNIPUB/ Kraus International Publication, 1981.

[2] Ross, P. J., Taguchi Techniques for Quality Engineering: Loss Function, Orthogonal Experiment, Parameter and Tolerance Design, McGraw-Hill, 1988, pp. 120–123.

[3] Manabe,K., Mori, S. and Suzuke, K., and Nishimura, H., Bulge forming of thin walled tubes by Micro-computer controlled hydraulic press, Advanced technology of plasticity, 1984 Vol.1, pp. 279-284.

[4] Manabe, K., Amino M., Effects of process parameters and material properties on deformation process in tube hydroforming, Journal of Materials Processing Technology ,2002,123, pp. 285–291.

[5] Mac Donald, B.J., Hashmi, M.S.J., Finite element simulation of bulge forming of a cross-joint from a tubular blank, Journal of Materials Processing Technology, 2000,103, pp. 333-342

[6] Ray, P., Mac Donald, B.J., Determination of the optimal load path for tube hydroforming processes using a fuzzy load control algorithm and finite element analysis. Finite Elements in Analysis and Design, 2004, 41, pp. 173–192

[7] Li, B., Nye, T.J. and Metzger, D. R., Multi-objective optimization of forming parameters for tube hydroforming process based on the Taguchi method, International Journal of Advanced Manufacturing Technology, 2006, 28, pp. 23–30.

[8] Li, B., Nye, T.J. and Metzger, D. R., Improving the reliability of the tube-hydroforming process by the Taguchi method, Transactions of the ASME, 2007, 129, pp.242-247

[9] Hallquist, J.O., LS-DYNA. Keyword User's Manual, Version 971, Livermore Software Technology Corporation, Livermore, 2007.

[10] Imaninejad, M., Subhash, G., and Loukus, A., Load Path Optimization of Tube Hydroforming Process, Int. J. Mach. Tools Manuf., 2005, 45, pp. 1504–1514.

[11] Al-Qureshi, H. A., and Moriera Filho, L. A., Junction Forming in Aluminum Tubes Using an Elastomer Technique, Mater. Manuf. Processes, 2001, 16, pp. 717–724.

[12] Stoughton, T.B., A general forming limit criterion for sheet metal forming, Int. J. Mech. Sci. 2000, 42, pp.1–27.

[13] Yoshida, K., Kuwabara, T., Narihara, K., Takahashi, S., Experimental verification of the path-independence of forming limit stresses, International Journal of Forming Processes, 2005, 8, pp. 283-298.

[14] Stoughton, T.B., Stress-based forming limits in sheet metal forming, Journal of Engineering Materials & Technology, Transactions of ASME, 2001, 123, pp. 417-422.

[15] Butuc, M.C., Gracio, J.J., Barata da Rocha, A., An experimental and theoretical analysis on the application of stress-based forming limit criterion, International Journal of Mechanical Sciences, 2006, 48, pp. 414-429.

[16] Green, D.E., Formability Analysis for Tubular Hydroformed Parts, Chapter 5 in Hydroforming for advanced manufacturing, Woodhead Publishing Ltd., Cambridge, England, ed. Koc, M., 2008, ISBN 978-1-84569-328-2

[17] Stoughton, T.B., Yoon, J. W., Sheet metal formability analysis for anisotropic materials under non-proportional loading, International Journal of Mechanical Sciences, 2005, 47, pp. 1972-2002.